Available online at www.sciencedirect.com
SCIENCE DIRECT®
Solid State Ionics 158 (2003) 141–150
SOLID STATE IONICS
www.elsevier.com/locate/ssi

Oxides of the AMO_3 and A_2MO_4-type: structural stability, electrical conductivity and thermal expansion

M. Al Daroukh[a], V.V. Vashook[a], H. Ullmann[a,*], F. Tietz[b], I. Arual Raj[c]

[a] *Institute of Inorganic Chemistry, Technical University of Dresden, Mommsenstr. 13, D-01062 Dresden, Germany*
[b] *Forschungszentrum Jülich GmbH, Institute for Materials and Processes in Energy Systems, D-52425 Jülich, Germany*
[c] *Central Electrochemical Research Institute, Karaikudi 630 006, Tamil Nadu, India*

Received 12 February 2002; received in revised form 23 August 2002; accepted 14 October 2002

Abstract

The structural and chemical stabilities, electrical conductivity, and thermal expansion of the $A_{2-a}A'_aMO_{4-x}$ oxides (A = La; A′ = Sr; M = Mn, Fe, Co, Ni) with the perovskite-related K_2NiF_4-type structure were investigated and compared with the characteristics of perovskite-type oxides AMO_{3-x} containing the same cations. The K_2NiF_4-type manganites, ferrites, cobaltites and nickelates are assumed to be reduction products of the corresponding perovskite-type oxides. The thermodynamic stabilities, in terms of reversible oxygen desorption, were higher than those of the corresponding perovskite-type oxides. Within the range of oxygen partial pressure (pO_2) from air to argon/H_2/H_2O, the oxidation states of the M cations were determined. The comparison of the oxidation states of M in AMO_{3-x} and (AMO_{3-x})·AO gives evidence on the stabilizing influence of the AO interlayer on the perovskite layer.

The electrical conductivity of the A_2MO_4 oxides was of p-type and reached values close to 100 S cm^{-1} at high oxygen partial pressures and 800 °C for nickelates and cobaltites. The thermal expansion of K_2NiF_4-type oxides is generally lower than that of the comparable perovskite-type oxides.

Keywords: Oxides; Perovskite structure; Chemical stability; Electrical conductivity; Oxygen transport; Thermal expansion

1. Introduction

Oxides of perovskite-type structure are important materials for a variety of electrical and catalytic applications. This structure type forms solid solutions with a lot of cations, which enables the alteration of the physical–chemical properties in a wide range. The transport of oxygen ions takes place via vacancies in the oxygen sublattice. There are many investigations on the composition–property relationship of AMO_3-type oxides with A = Ln (lanthanides), Ca, Sr, Ba; M = Cr, Mn, Fe, Co, Ni, Ga, In, with mixed occupation of the A- and M-sublattices. For these compositions, several applications such as oxide electrodes [1–3], electrolytes [4], catalysts [1,5], oxygen separation membranes [6] and magnetoresistant materials [7] were considered.

In zirconia-based solid oxide fuel cells (SOFCs), cathodes of the composition $La_{1-a}Sr_aMnO_{3-x}$ are

* Corresponding author. Tel.: +49-351-463-4792; fax: +49-351-463-7752.
E-mail address: helmut.ullmann@chemie.tu-dresden.de (H. Ullmann).

0167-2738/02/$ - see front matter © 2002 Elsevier Science B.V. All rights reserved.
PII: S0167-2738(02)00773-7

Table 1
Solid state reaction conditions and composition ranges of A_2MO_4-type oxides

Composition	Annealing temperature in air (°C)	Range of Sr concentration (solid solution)	Reference
$La_{2-a}Sr_aMnO_{4\pm x}$	1350	$1.2 < a < 1.5$	this work
$La_{2-a}Sr_aFeO_{4\pm x}$	1200	$1.0 < a < 1.3$	[24]
$La_{2-a}Sr_aCoO_{4\pm x}$	1200	$0.5 < a < 1.5$	[15]
$La_{2-a}Sr_aNiO_{4\pm x}$	1400	$0 < a < 1.5$	[14]

applied [8,9]. For future SOFCs operating at about 700 °C, new oxide electrodes based on ferrites and cobaltites with higher electrocatalytic activity were proposed [10]. The electrocatalytic activity of the oxides is determined by the electronic band structure, both the electronic and the oxide ionic conductivities and the surface exchange properties. Additionally, practical applicability requires phase purity, chemical stability and thermal expansions adjusted to the materials combinations of the fuel cell. However, materials with the best electrocatalytic characteristics such as $La_{1-a}Sr_aFe_{1-b}Co_bO_{3-x}$ were found to have low chemical stability and unacceptably high thermal expansion for $0.4 < a < 1$ and $0.5 < b < 1$ [6,11].

A_2MO_4 oxides with the perovskite-related K_2NiF_4-type structure are less intensively investigated. Recent results on lanthanum cobaltites and nickelates [12–19] indicated enhanced chemical stability and moderate thermal expansion. The ideal K_2NiF_4-type structure represents a combination of the AMO_3 perovskite and AO rock-salt layers arranged one upon the other [20,21].

The aim of this work was to investigate systematically $A_{2-a}A_a'MO_{4-x}$-type oxides with A = Ln, A′ = Sr, M = Mn, Fe, Co, Ni and to compare the structural and chemical stabilities, electrical conductivity, and thermal expansion with the characteristics of perovskite-type oxides AMO_{3-x} being composed of the same cations.

2. Fundamental

Corresponding to the thermodynamic stabilities of the oxides within the range of phase stability, the oxide AMO_3 undergoes a partial reduction/oxidation reaction resulting in the well-known oxygen vacancy and electron hole-type defect structure, which determines the electrical transport properties of the oxides.

$$AMO_3 = AMO_{3-x} + x/2\ O_2 \quad (1)$$

At higher temperatures and lower oxygen partial pressures, the AMO_3 phase becomes unstable and reacts to A_2MO_4:

$$2\ AMO_3 = A_2MO_4 + MO + 1/2\ O_2 \quad (2)$$

Reaction (2) can be assumed as a proof of the higher thermochemical stability of the A_2MO_4-type compounds compared with the AMO_3-type oxides. A_2MO_4-type oxides undergo partial reduction/oxidation reactions as well, corresponding to their thermodynamic stabilities within the range of existence of the phase.

$$A_2MO_4 = A_2MO_{4\pm x} \pm x/2\ O_2 \quad (3)$$

The regular oxygen sites within the K_2NiF_4-type structure are completely occupied at an oxygen

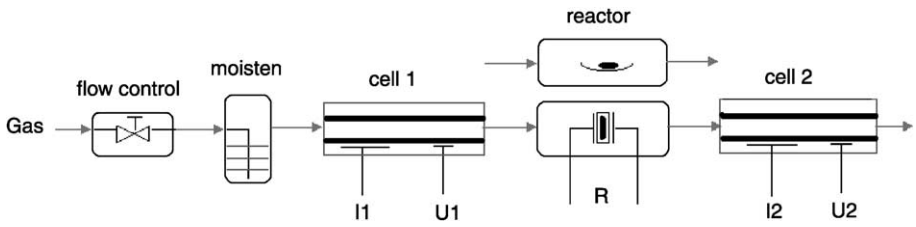

Fig. 1. Schematic view of the solid electrolyte device OXYLYT. I1, I2 are the electrolytic current in cell 1 and cell 2, while U1, U2 represent the voltage of cell 1 and cell 2.

Table 2
Results of chemical analysis of the O/M stoichiometries of the initial samples as prepared in air

Composition K_2NiF_4-types	O/M stoichiometry as determined by		Assumption: as in cobaltites
	Total reduction	Iodometry (#) or cerimetry (§)	
$La_{1.4}Sr_{0.6}CoO_{4\pm x}$	4.05		
$La_{1.3}Sr_{0.7}CoO_{4\pm x}$	4.03		
$LaSrCoO_{4\pm x}$	4.00		
$La_{0.8}Sr_{1.2}CoO_{4\pm x}$	3.95		
$La_2NiO_{4\pm x}$	4.16	4.14 (#)	
$La_{1.7}Sr_{0.3}NiO_{4\pm x}$	4.10	4.09 (#)	
$La_{1.4}Sr_{0.6}NiO_{4\pm x}$	4.03	4.03 (#)	
$LaSrFeO_{4\pm x}$	no analysis	no analysis	4.00
$La_{0.8}Sr_{1.2}FeO_{4\pm x}$	no analysis	no analysis	3.95
$La_{0.5}Sr_{1.5}MnO_{4\pm x}$		3.99 (§)	

stoichiometry of 4.0. In compositions with $A+A'>1$ excess oxygen ions may occupy interstitial oxygen sites as demonstrated by structure investigations [22,23].

The perovskite and the K_2NiF_4-type oxide phases are characterized by a range of existence expressed by the O/M stoichiometry range $(3-x)$ and $(4-x)$, respectively. Therefore, one fixed value for the free energy, ΔG^{o}, does not exist. Within the range of existence of the phases, the value x of reversible oxygen exchange according to reactions (1) and (3) is used as an expression for the thermodynamic stability.

$$x = f(T, pO_2) \tag{4}$$

3. Experimental

3.1. Preparation and phase characterization

Powders of A_2BO_4 oxides were prepared by solid state reaction from La_2O_3, $SrCO_3$, Mn_2O_3, Fe_2O_3, Co_3O_4 and NiO of 99.9% purity in air by a two-step treatment. The initial powders were mixed in a planetary mill and heated at 1000 °C in air for 6 h. The products were crushed, ground and heated at 1200–1350 °C for 24 h. The preparation of the perovskite powders by solid state reaction was described in Ref. [11]. The maximum sintering temperature was 1250 °C.

Quantitative chemical analysis of the cationic compositions of some samples was carried out by atomic absorption spectroscopy (AAS-3 spectrometer, Carl Zeiss Jena). The cation ratios were found to be equal to the stoichiometric ratios of the initial mixtures with accuracy better than ± 0.01 mol.

Structure and phase compositions were checked by X-ray diffractograms of the powders by means of Cu K_α radiation in a Siemens D5000 device. After the solid

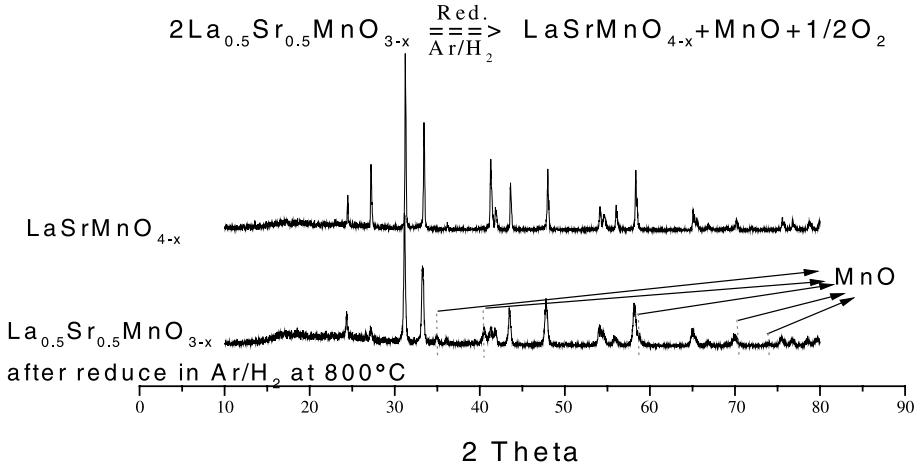

Fig. 2. Comparison of the XRD patterns of $LaSrMnO_4$ (top) and of $La_{0.5}Sr_{0.5}MnO_{3-x}$ (after reduction in Ar/H_2 (bottom)).

state reaction in air, single-phase $La_{2-a}Sr_aNiO_{4\pm x}$ nickelates of the K_2NiF_4-type structure were formed with $0<a<1.5$ [14], the $La_{2-a}Sr_aCoO_{4\pm x}$ cobaltites with $0.5<a<1.5$ [15]. Analogously, the $La_{2-a}Sr_aFeO_{4\pm x}$ ferrites were formed in the range $1.0<a<1.3$ [24]. $La_{2-a}Sr_aMnO_{4\pm x}$ with Sr <1.2 was only

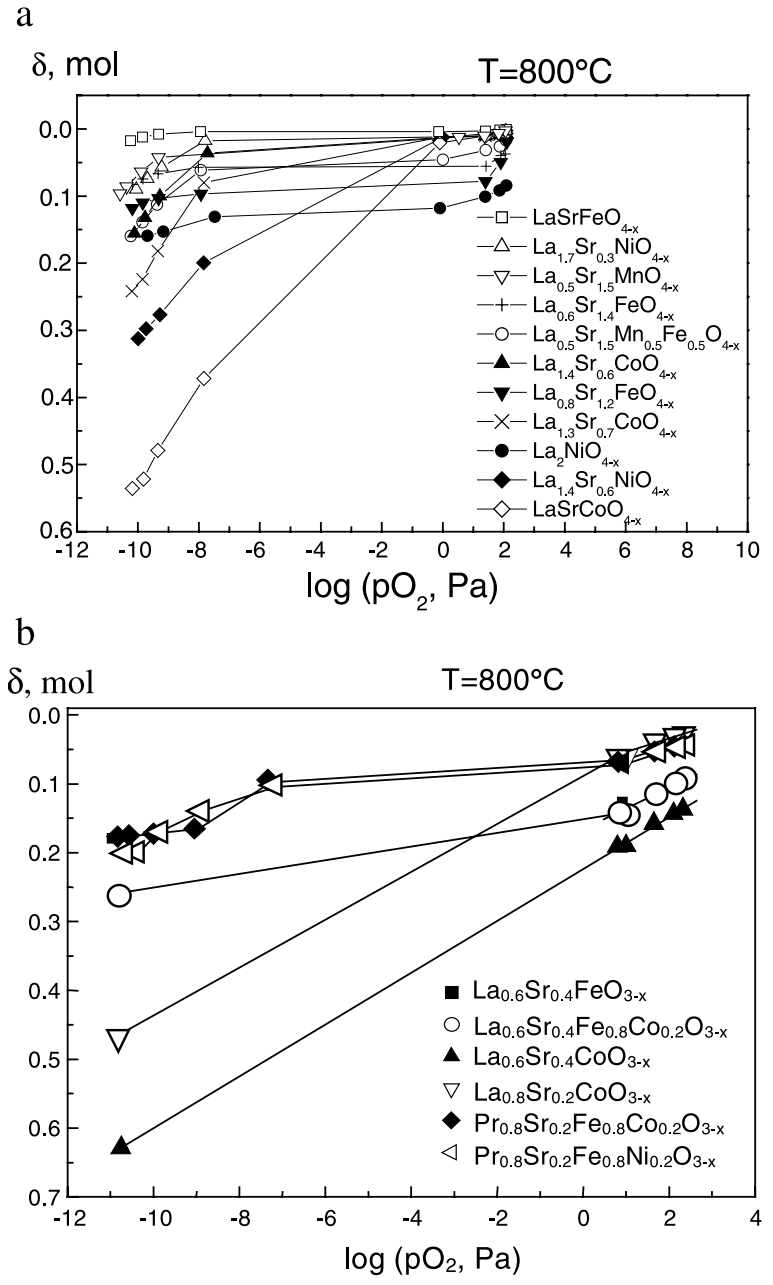

Fig. 3. Released oxygen δ of the air-treated oxide powders after equilibration in Ar/O_2 and $Ar/H_2/H_2O$ at a temperature of 800 °C. (a) K_2NiF_4-type oxides, after Ref. [28], (b) perovskite-type oxides, after Refs. [11,28].

stable in an atmosphere with reduced oxygen content. With increasing stability of the transition metal oxide MO (Ni < Co < Fe < Mn) the ranges of existence (in air) of the Sr-substituted $La_{2-a}Sr_aMO_{4\pm x}$ phases shift to higher Sr concentrations along this row (Table 1).

For preparation of ceramic specimens, the powders were pressed and sintered at 1200–1500 °C for 20 h. The ceramic samples were gastight except for the $La_{2-a}Sr_aCoO_{4-x}$ samples. The relative densities of the gastight samples were determined by means of a pycnometer and were found greater than 93% of the theoretical density. Theoretical densities were calculated from the unit cell dimensions, the molar weight and the number of formula units per unit cell.

3.2. Oxygen stoichiometry measurements

Oxygen deficiencies of the oxides were measured on powders placed in a quartz container within the furnace of a solid electrolyte device OXYLYT [25] (Fig. 1). A steady stream of argon with a controlled oxygen partial pressure (pO_2) sensored by cell 1 flowed through the sample furnace. Gases of controlled pO_2 (investigated range: 10^{-10}–10^4 Pa) were prepared from argon/oxygen or argon/hydrogen/water vapour mixtures; the pO_2 values were modified within the oxidizing and reducing regions by subsequent electrolytic pumping (current I of cell 1). The corresponding pO_2 values were measured by a solid electrolyte potentiometric cell (potential U_1 of cell 1). After reaction with the sample, the deviation of the oxygen content from the initial state is detected by cell 2.

Both chemical analysis and total reduction of the compounds was used to identify the initial state of the oxygen-to-metal stoichiometry. The chemical analysis of the Mn-based oxides was performed by cerimetric titration in H_2SO_4 solution. The Mn^{3+} and Mn^{4+} oxidize Fe^{2+} to Fe^{3+}. The excess of Fe^{2+} ions is retitrated by a Ce^{4+} solution. The initial oxygen-to-metal stoichiometries of Co and Ni-based oxides were determined after total reduction of the complex oxides to La_2O_3, SrO, and metallic Co, or Ni, respectively. The reduction was performed by heating in a flow of dry Ar/5% H_2 mixture at 900–1000 °C. The completeness of reduction was controlled by the solid electrolyte device and by X-ray diffractometry. For Fe-based oxides, none of these analyses were applicable. Results are given in Table 2.

3.3. Measurements of electrical conductivity

The electrical conductivity was measured on air-sintered samples of 2 × 4 × 10 mm in size by a four-point DC measurement. Before pressing, the shapes were equipped with four platinum wires (0.1 mm diameter). The temperature dependence was measured in air during steady cooling (3 °C/min) from 1000 down to 200 °C. During measurements in gases of lower pO_2, the equilibrium values of conductivity were used after stepwise heating and cooling.

3.4. Thermal expansion measurements

The relative thermal expansion from room temperature to 1000 °C was measured in air and in argon on air-sintered rectangular ceramic sticks of 25 × 6 × 6 mm with polished frontal faces using a NETZSCH 402C dilatometer. Heating and cooling rates were 3 K/min with an annealing time of 1 h at maximum temperature. Measurements in argon (5–130 Pa O_2) were performed in flowing gas.

Table 3
Average oxidation states ($m+$) of M cations of the perovskite AMO_{3-x} and the perovskite-related A_2MO_{4-x} compositions, calculated from oxygen deficiencies δ as function of oxygen partial pressures pO_2 at 800 °C

Composition	$m+$ at log (pO_2, Pa)			$\Delta m+ = \pm 0.005$		
log pO_2=	2	1	−1	−7	−8	−10
ABO_{3-x}						
$La_{0.6}Sr_{0.4}FeO_{3-x}$	3.18	3.12				3.04
$La_{0.6}Sr_{0.4}CoO_{3-x}$	3.12	3.04	3.00			2.30
$La_{0.8}Sr_{0.2}CoO_{3-x}$	3.15	3.10	3.00			2.40
$La_{0.5}Sr_{0.5}MnO_{3-x}$	3.34	3.33	3.32	3.30	3.28	3.25
$Pr_{0.8}Sr_{0.2}Fe_{0.8}Ni_{0.2}O_{3-x}$	3.04	3.0	2.96	2.92	2.87	2.85
$Pr_{0.5}Sr_{0.5}Fe_{0.8}Co_{0.2}O_{3-x}$	3.06	3.0	2.99	2.99	2.99	2.90
A_2BO_{4-x}						
$La_{1.4}Sr_{0.6}NiO_{4-x}$	2.66	2.65	2.60	2.31	2.26	2.04
$La_{1.7}Sr_{0.3}NiO_{4-x}$	2.54	2.54	2.53	2.52	2.51	2.38
La_2NiO_{4-x}	2.17	2.13	2.10	2.08	2.06	2.01
$La_{1.4}Sr_{0.6}CoO_{4-x}$	2.93	2.92	2.91	2.88	2.85	2.65
$LaSrCoO_{4-x}$	2.88	2.86	2.77	2.22	2.12	1.83
$LaSrFeO_{4-x}$	3.00	2.99	2.99	2.99	2.99	2.97
$La_{0.8}Sr_{1.2}FeO_{4-x}$	3.06	2.94	2.93	2.91	2.90	2.87
$La_{0.5}Sr_{1.5}MnO_{4-x}$	3.49	3.48	3.47	3.43	3.42	3.37

4. Results and discussion

4.1. Chemical stability

The stability of the oxides with the perovskite-type structure after reaction (1) was investigated in Refs. [11,26,27]. The formation of the K_2NiF_4-type oxides after reduction of perovskites by reaction (2) was demonstrated for $La_{0.5}Sr_{0.5}MnO_3$ annealed in Ar/H_2 at 800 °C. Besides the K_2NiF_4 pattern the reflections of MnO were visible in the X-ray diffractogram [28] (Fig. 2).

The reduction stability of the K_2NiF_4-type oxides was tested in $Ar/H_2/H_2O$ ($pO_2 = 10^{-11}$ Pa) and Ar/5% H_2. Phase stability was indicated by identical XRD patterns of the air-treated and the argon-treated states. In $Ar/H_2/H_2O$ at 800 °C, all compositions remained stable. In Ar/H_2 the cobaltites and nickelates were decomposed, only the ferrites and manganites remained stable.

As a value of the thermodynamic stability after Eq. (4) the O/M stoichiometry is defined. Starting from air-treated $A_{2-a}A'_aMO_{4\pm x}$ (air) oxides the amounts δ of oxygen are released during equilibration in Ar/O_2 and $Ar/H_2/H_2O$ at a temperature of 800 °C (Fig. 3a). $LaSrFeO_{4-x}$, $La_{1.7}Sr_{0.3}NiO_{4-x}$ and $La_{0.5}Sr_{1.5}MnO_{4-x}$ represent high stability according to low oxygen release up to oxygen partial pressures of 10^{-10} Pa. The stabilities of the ferrites with strontium content >1 are lower. Fe substitution for Mn decreases the stability of the manganite. Nickelate of lower or higher Sr content have lower stability compared to $La_{1.7}Sr_{0.3}NiO_4$. The cobaltites have generally low stabilities indicated by high oxygen release of the air-treated samples.

For comparison, the oxygen released from perovskite-type oxides within the range of their existence after reaction (1) is given in Fig. 3b (after Ref. [27]). The amount of released oxygen increases from manganites to ferrites to cobaltites, and additionally with increasing Sr concentration on A-site and with Ni on B-site. This sequence is in accordance with the stabilities of the transition metal oxides of the M cations. Comparing the oxygen release of the perovskite oxides and the K_2NiF_4-type oxides of nearly comparable La/Sr ratios and similar M cations, the values of δ are always higher for the perovskite-type, indicating lower stabilities of this type of structure.

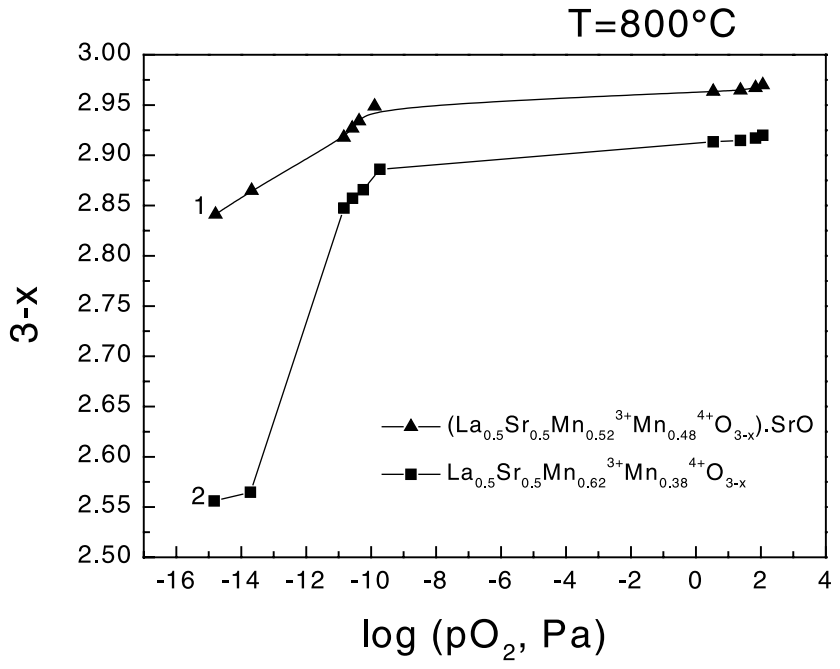

Fig. 4. O/M stoichiometries of the perovskite-type oxide $La_{0.5}Sr_{0.5}MnO_{3-x}$ (2) and the layered perovskite-type oxide $(La_{0.5}Sr_{0.5}MnO_{3-x})\cdot SrO$ (1).

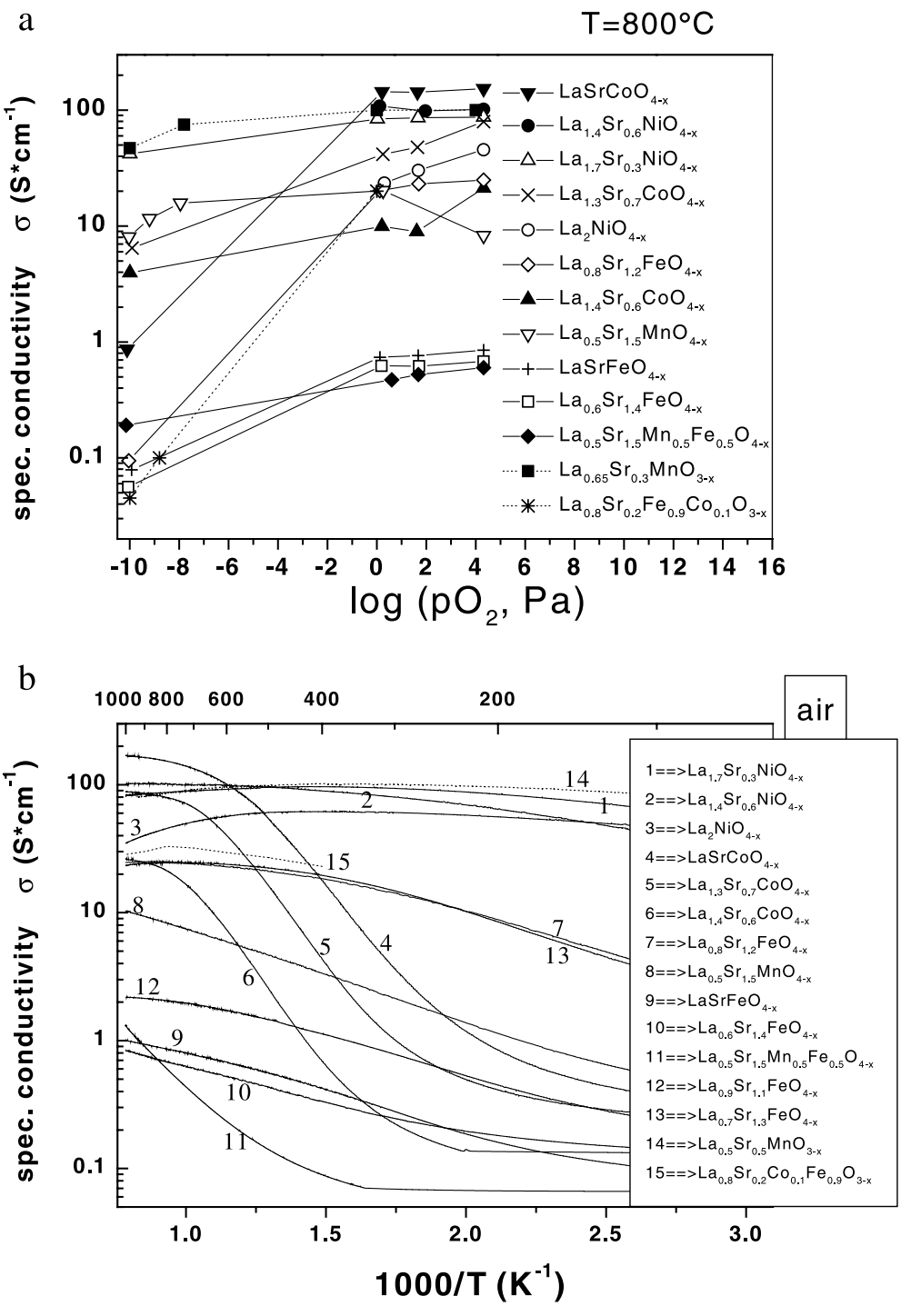

Fig. 5. Specific electrical conductivity of A_2MO_4 oxides. (a) Dependence on oxygen partial pressure at 800 °C, (· · ·) perovskite-type oxides, (b) dependence on temperature in air, (· · ·) perovskite-type oxides.

To calculate the average oxidation states (m+) of the M cations, the measured values δ were subtracted from the initial oxygen-to-metal (O/M) stoichiometries of the air-treated samples ($4 \pm x_{air}$) to obtain the oxygen-to-metal stoichiometries as function of pO_2, as given in Table 2: $(4 \pm x)=(4 \pm x_{air} - \delta)$. The average oxidation states of M cations in $A_{1-a}A'_aMO_{3-x}$ and in $A_{2-a}A'_aMO_{4-x}$ at 800 °C versus log pO_2 are given in Table 3. Within the pO_2 range investigated, the oxidation state of the Mn ions in both types of oxide structures is higher than 3+. In Fe-based $A_{2-a}A'_aMO_{4-x}$ oxides at Sr = 1, the average oxidation state of Fe is 3+. In cobaltites and nickelates, the oxidation state of the M cations is always <3+, decreasing with decreasing Sr content. In La_2NiO_{4-x}, nearly the 2+ state for Ni is reached. The extraordinary stable composition $La_{1.7}Sr_{0.3}NiO_{4-x}$ is characterized by an oxidation state of about 2.5 for Ni, which means $[Ni^{2+}] \approx [Ni^{3+}]$.

The comparison of the oxidation states of AMO_{3-x} and AMO_{3-x}·AO gives evidence on the stabilizing influence of the AO interlayer on the perovskite layer. Comparable compositions of the perovskite and the perovskite-layered structure show higher O/M stoichiometries at low oxygen partial pressures for the layered structures, e.g. for $La_{0.5}Sr_{0.5}MnO_{3-x}$ and $La_{0.5}Sr_{0.5}MnO_{3-x}$·SrO (Fig. 4), demonstrating higher thermodynamic stability of the latter oxide.

4.2. Electrical conductivity

The electrical conductivities of the A_2MO_4 oxides at 800 °C as function of the oxygen partial pressure are summarised in Fig. 5a. At high oxygen partial pressures, the highest conductivities—nearly 100 S cm^{-1}—were measured for nickelates and cobaltites. Below 1 Pa of oxygen, the conductivities decreased for the less stable Co- and Ni-based oxides as it is typical of p-type semiconductivity. The decrease is less rapid than for comparable oxides of the perovskite-type [11]. Especially, the composition $La_{1.7}Sr_{0.3}NiO_{4-x}$ shows high p-type conductivity down to oxygen partial pressures of 10^{-10} Pa. The conductivity of this composition at 800 °C within the whole pO_2 range is as high as the values of the recently used cathode materials based on perovskite-type manganites. The conductivities of the Fe- and Mn-based oxides of the A_2MO_4-type within the range of cathodic pO_2 values are lower than the conductivities of the perovskite-type oxides with the same cations [11].

The electrical conductivities in air of the A_2MO_4 oxides increase with temperature, indicating thermally activated semiconductivity (Fig. 5b). The specific conductivities of the A_2MO_4-type nickelates are high (80–100 S cm^{-1}) within the whole temperature region between 200 and 1000 °C. The cobaltites (with 1 and 0.7 mol Sr) accomplished comparable values above 600 °C. The ferrites with 1.2 and 1.3 mol Sr show already rather low values of conductivity (10–25 S cm^{-1}) in air at 400–1000 °C. Ferrites with higher or lower Sr content are poor electrical conductors. The manganite with high Sr content (1.5 mol) reached values of only 10 S cm^{-1} at temperatures above 800 °C. The conductivity values of the perovskite oxides $La_{0.5}Sr_{0.5}MnO_{3-x}$ (curve 14) and $La_{0.8}Sr_{0.2}Fe_{0.9}Co_{0.1}O_{3-x}$ (curve 15) may serve as lower limits for the required conductivity of the electrodes in SOFCs.

4.3. Thermal expansion

Values of thermal expansion coefficients of K_2NiF_4-type oxides and perovskite-type oxides are collected in Table 4. The thermal expansion coefficients of K_2NiF_4-type oxides are generally lower than the coefficients of the perovskite-type oxides of comparable cationic compositions. The difference in thermal expansion

Table 4
Thermal expansion in air and argon of complex oxides

Composition	TEC (30–1000 °C) × 10^6 K^{-1}	
	Air	Argon/O_2
A_2BO_{4-x}		
$La_{1.3}Sr_{0.7}CoO_{4-x}$	9.6 [19]	9.5 [19]
$LaSrCoO_{4-x}$	14.3	14.5
$La_{0.9}Sr_{1.1}FeO_{4-x}$	12.7	12.9
$La_{1.7}Sr_{0.3}NiO_{4-x}$	11.3 [19]	12.0 [19]
$La_{1.6}Sr_{0.4}NiO_{4-x}$	13.2	13.4
$La_{1.4}Sr_{0.6}NiO_{4-x}$	11.0 [19]	12.0 [19]
La_2NiO_{4-x}	11.9	11.6
ABO_{3-x}		
$La_{0.65}Sr_{0.3}Fe_{0.8}Co_{0.2}O_{3-x}$	15.2	18.8
$Sr_{0.9}Ce_{0.1}Fe_{0.5}Co_{0.5}O_{3-x}$	22.6	23.8
$La_{0.6}Sr_{0.4}FeO_{3-x}$	16.3 [29]	–
$La_{0.6}Sr_{0.4}Fe_{0.8}Co_{0.2}O_{3-x}$	17.5 [11]	–
$La_{0.8}Sr_{0.2}Fe_{0.9}Co_{0.1}O_{3-x}$	13.9 [11]	–
$Pr_{0.8}Sr_{0.2}Fe_{0.8}Co_{0.2}O_{3-x}$	13.2	14.0
$Ce_{0.1}Sr_{0.9}Fe_{0.8}Ni_{0.2}O_{3-x}$	18.9 [11]	–

between measurements in air and in argon environment are smaller for K_2NiF_4-type oxides compared with the differences for the AMO_3 oxides.

5. Conclusions

The K_2NiF_4-type manganites, ferrites, cobaltites and nickelates can be regarded as reduction products of the corresponding perovskite-type oxides. Their thermodynamic stability is higher than those of the corresponding perovskite-type oxides. Within the pO_2 range from air to argon/H_2/H_2O, the oxidation state of the M cations in $A_{2-a}A'_aMO_{4-x}$ is higher than in the corresponding perovskite-type oxides. The oxidation state of the M cations decrease from Mn (>3+) via Fe, Co to Ni (<3+). $La_{1.7}Sr_{0.3}NiO_{4-x}$ with Ni=+2.5 is very stable. The comparison of the oxidation states of AMO_{3-x} and $(AMO_{3-x})\cdot AO$ gives evidence on the stabilizing influence of the AO interlayer on the perovskite layer. The electrical conductivities of the A_2MO_4 oxides are of p-type and reach nearly 100 S cm^{-1} at 800 °C and high oxygen partial pressures for nickelates and cobaltites. At lower oxygen partial pressures the conductivities decrease for the less stable Co- and Ni-based oxides, but less rapidly than for comparable perovskite oxides. The thermal expansion of K_2NiF_4-type oxides is generally lower than that of the perovskite-type oxides of comparable cationic compositions.

Acknowledgements

The authors are grateful to Deutsche Forschungsgemeinschaft and to Friedrich-Ebert-Stiftung, Bonn/Germany for financial support. Part of this work was carried out in the frame of the German–Indian bilateral scientific project (No. IND 99/043) supported by the German Ministry of Science and Education, Berlin/Bonn, and the Indian Council of Scientific and Industrial Research (CSIR), New Delhi.

References

[1] M.A. Peca, J.L.G. Fierro, Chem. Rev. 101 (2001) 1981–2017.
[2] G. Pudmich, B.A. Boukamp, M. Gonzales-Cuenza, W. Jungen, F. Tietz, Solid State Ionics 135 (2000) 433–438.
[3] L.W. Tai, M.M. Nasrallah, H.U. Proc. 3rd Int. Symp. Solid Oxide Fuel Cells (SOFC-III), in: S.C. Singhal, H. Iwahara (Eds.), Electrochem. Soc. Proc., vols. 93–94, 1993, p. 241.
[4] T. Ishihara, H. Matsuda, Y. Takita, J. Am. Chem. Soc. 116 (1994) 3801–3803.
[5] U. Balachandran, J.T. Dusek, S.M. Sweeney, R.B. Poeppel, R.L. Mieville, P.S. Maiya, M.S. Kleefisch, S. Pei, T.P. Kobylinski, C.A. Udovich, A.C. Bose, Am. Ceram. Soc. Bull. 74 (1995) 71–75.
[6] A. Petric, R. Peng Huang, F. Tietz, Solid State Ionics 135 (2000) 719–725.
[7] Y. Moritomo, A. Asamitsu, H. Kuwahara, Y. Tokura, Nature 380 (1996) 141.
[8] H.U. Anderson, Solid State Ionics 52 (1992) 33–41.
[9] A. Ahmad-Khanlou, F. Tietz, I.C. Vinke, D. Stöver, in: H. Yokokawa, S.C. Singhal (Eds.), Proc. 7th Int. Symp. Solid Oxide Fuel Cells (SOFC-VII), The Electrochemical Society, Pennington, NJ, 2001, pp. 476–484.
[10] R. Doshi, V.L. Richards, M. Krumpelt, Solid oxide fuel cells V, in: U. Stimming, S.C. Singhal, H. Tagawa, W. Lehnert (Eds.), Proc. of the Fifth Int. Symposium, Aachen, Germany, 1997, p. 379.
[11] H. Ullmann, N. Trofimenko, F. Tietz, D. Stöver, A. Ahmad-Khanlou, Solid State Ionics 138 (2000) 79–90.
[12] V.V. Vashook, O.P. Olshevskaya, H. Ullmann, N. Trofimenko, R. Soltis, D. Thomson, 6th Int. Symp. Systems with Fast Ionic Transport, Cracow, Poland, 9–12 May 2001, 2001, pp. VI-P3, Extended Abstracts.
[13] V.V. Kharton, A.A. Yaremchenko, E.N. Naumovich, J. Solid State Electrochem. 3 (1999) 303–326.
[14] V.V. Vashook, I.I. Yushkevich, L.V. Kokhanovsky, L.V. Makhnach, S.P. Tolochko, I.F. Kononyuk, H. Ullmann, H. Altenburg, Solid State Ionics 119 (1999) 23–30.
[15] V.V. Vashook, H. Ullmann, O.P. Olschevskaya, V.P. Kulik, M.E. Lukaschevich, L.V. Kochanovskij, Solid State Ionics 138 (2000) 99–104.
[16] S.J. Skinner, J.A. Kilner, Solid State Ionics 135 (2000) 709–712.
[17] S.P. Tolochko, I.F. Kononyuk, S.F. Strelcak, E.A. Korzyuk, Wesci AN BSSR Ser. Chim. Nauk 4 (1984) 67–70 (in Russian).
[18] V.V. Vashook, S.P. Tolochko, I.I. Yushkevich, L.V. Makhnach, I.F. Kononyuk, H. Altenburg, J. Hauck, H. Ullmann, Solid State Ionics 110 (1998) 245–253.
[19] V.V. Vashuk, Synthesis and physico-chemical properties of compounds of the perovskite and perovskite-like structures on the basis of cobaltates and nickelates, Thesis, National Acad. Sci. of Belarus, Minsk, Sept. 2000 (in Russian).
[20] G. Flem, G. Demazeau, P. Hagenmuller, J. Solid State Chem. 44 (1982) 82–88.
[21] K.K. Singh, P. Ganguly, Spectrochim. Acta 40A (1984) 539–545.
[22] J.D. Jogensen, B. Dabrowsky, Sh. Pei, Phys. Rev., B 40 (1989) 2187–2191.
[23] Z. Hiroi, M. Takano, Y. Bondo, Supercond. Sci. Technol. 4 (1991) 139–141.
[24] T. Omata, K. Ueda, H. Hosono, M. Katada, N. Ueda, H. Kawazoe, Phys. Rev., B 49 (1994) 10194–10199.

[25] K. Teske, H. Ullmann, N. Trofimenko, J. Therm. Anal. 49 (1997) 1211–1220.
[26] N. Trofimenko, H. Ullmann, Oxygen deficiency of perovskite-type oxides $A_{1-a}A'_aB_{1-b}B'_bO_{3-a/2+\delta}$ (A = La,Ce, Pr; A′ = Sr; B,B′ = Mn,Fe,Co,Ni) (in preparation).
[27] N.E. Trofimenko, H. Ullmann, J. Eur. Ceram. Soc. 20 (2000) 1241–1250.
[28] M. Al Daroukh, Thermodynamic stability and electrical properties of oxide materials with the perovskite and perovskite-related K_2NiF_4 structures, PhD Thesis, Technical University Dresden, Fac. Nat. Math., 2001.
[29] L. Kindermann, F.W. Poulsen, P.H. Larsen, H. Nickel, K. Hilpert, in: Ph. Stevens (Ed.), Proc. 3rd Eur. SOFC Forum, vol. 2, 1998, pp. 123–132, Nantes, France.